

Article

CO₂ Recycling in the Iron and Steel Industry via Power-to-Gas and Oxy-Fuel Combustion

Jorge Perpiñán ¹, Manuel Bailera ^{1,2}, Luis M. Romeo ^{1,*}, Begoña Peña ¹ and Valerie Eveloy ³

¹ Escuela de Ingeniería y Arquitectura, Universidad de Zaragoza, María de Luna 3, 50018 Zaragoza, Spain; jorge.perpinan@unizar.es (J.P.); mbailera@unizar.es (M.B.); bpp@unizar.es (B.P.)

² Graduate School of Creative Science and Engineering, Waseda University, Tokyo 169-8555, Japan

³ Department of Mechanical Engineering, Khalifa University, Abu Dhabi P.O. Box 127788, United Arab Emirates; valerie.eveloy@ku.ac.ae

* Correspondence: luismi@unizar.es

Abstract: The iron and steel industry is the largest energy-consuming sector in the world. It is responsible for emitting 4–5% of the total anthropogenic CO₂. As an energy-intensive industry, it is essential that the iron and steel sector accomplishes important carbon emission reduction. Carbon capture is one of the most promising alternatives to achieve this aim. Moreover, if carbon utilization via power-to-gas is integrated with carbon capture, there could be a significant increase in the interest of this alternative in the iron and steel sector. This paper presents several simulations to integrate oxy-fuel processes and power-to-gas in a steel plant, and compares gas productions (coke oven gas, blast furnace gas, and blast oxygen furnace gas), energy requirements, and carbon reduction with a base case in order to obtain the technical feasibility of the proposals. Two different power-to-gas technology implementations were selected, together with the oxy blast furnace and the top gas recycling technologies. These integrations are based on three strategies: (i) converting the blast furnace (BF) process into an oxy-fuel process, (ii) recirculating blast furnace gas (BFG) back to the BF itself, and (iii) using a methanation process to generate CH₄ and also introduce it to the BF. Applying these improvements to the steel industry, we achieved reductions in CO₂ emissions of up to 8%, and reductions in coal fuel consumption of 12.8%. On the basis of the results, we are able to conclude that the energy required to achieve the above emission savings could be as low as 4.9 MJ/kg CO₂ for the second implementation. These values highlight the importance of carrying out future research in the implementation of carbon capture and power-to-gas in the industrial sector.

Citation: Perpiñán, J.; Bailera, M.; Romeo, M.L.; Peña, B., Eveloy, V. CO₂ Recycling in the Iron and Steel Industry via Power to Gas and Oxy-Fuel Combustion.

Energies **2021**, *14*, x.

<https://doi.org/10.3390/xxxxx>

Academic Editor: Attilio Converti

Received: 27 September 2021

Accepted: 22 October 2021

Published: date

Keywords: ironmaking; power-to-gas; iron and steel industry; methanation; oxy-fuel combustion; top gas recycling

Publisher's Note: MDPI stays neutral with regard to jurisdictional claims in published maps and institutional affiliations.



Copyright: © 2021 by the authors. Submitted for possible open access publication under the terms and conditions of the Creative Commons Attribution (CC BY) license (<http://creativecommons.org/licenses/by/4.0>)

1. Introduction

The iron and steel sector is one of the most energy- and carbon-intensive in the world. Iron and steel making processes are still mostly coal-based and thus highly dependent on fossil fuels, releasing a substantial amount of CO₂ [1]. According to the Intergovernmental Panel on Climate Change (IPCC), the steel industry accounts for 4–5% of the total world CO₂ emission. It is the second largest consumer of industrial energy, consuming around 616 Mtoe (25.8 EJ) [2].

The iron and steel industry has a complex structure. However, only a limited number of processes are used worldwide that use similar energy resources and raw materials. Globally, steel is produced using two main routes, the blast furnace–basic oxygen furnace route (BF-BOF) and the direct scrap smelting route (electric arc furnace (EAF)). The BF-BOF route uses mainly iron ore, and depending on the facility, up to 30% scrap.

The EAF route mainly uses scrap, and depending on the facility, up to 30% iron and iron ore [2–4].

Another fundamental difference between the two routes is the nature of the energy input. In the case of the BF-BOF, mainly coke is used as fuel, while the EAF route produces steel using mainly recycled steel and electricity. The overall process of the two main steel production routes is depicted in Figure 1.

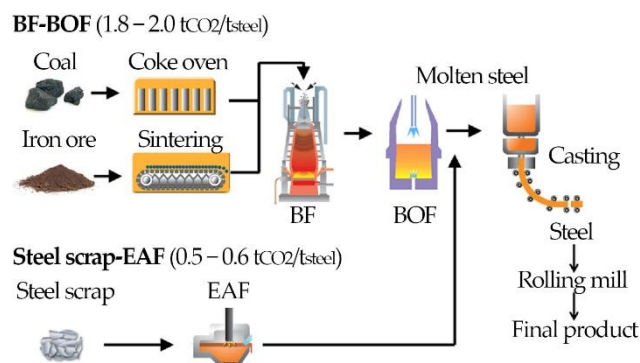
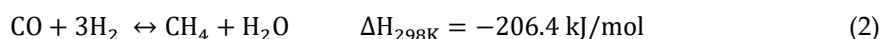


Figure 1. Main routes of steel production [4].

The BF-BOF route consists of several processes: sintering, coke oven, blast furnace, basic oxygen furnace, and the final stage of casting and rolling. The sintering is used to agglomerate iron ore. The coke oven allows for the obtaining of coke from coal by pyrolysis. In the BF, the iron ore is reduced by coke obtaining pig iron, then the BOF lowers the carbon content of the iron thus obtaining steel, and finally the hot metal passes through casting and rolling to obtain the final desired form. Along this processes, different waste exhaust fuel gases are obtained, which can be used in the steel plant (coke oven gas (COG), blast furnace gas (BFG), and basic oxygen furnace gas (BOFG)). All of them contain CO₂, which is emitted into the atmosphere unless the waste gas is recycled and/or treated.

A third iron and steel production route, the direct reduced iron (DRI)-EAF route, uses natural gas or coal-based syngas as reducing agent in combustion-free reactors to directly reduce the iron ore into metallic iron, which is processed in EAFs to produce steel. DRI processes differ in terms of the iron source (fine ore or pellets) and reactor type (fluidized bed, fixed bed, or shaft furnace). Among them, the commercially available Energiron and Midrex concepts, which use iron pellets in shaft furnaces with countercurrent moving beds, are the best options from an environmental point of view. Although representing significantly smaller steel production market shares than either the BF-BOF or EAF routes, DRI-EAF has the potential for significant carbon abatement.

Aiming for solutions that substantially reduce CO₂ while providing additional benefits, power-to-gas (PtG) stands out as a promising candidate [5]. The PtG concept converts renewable electricity into valuable gases using an electrolysis stage and uses CO₂ that may come from industrial processes. Conventionally, the conversion of electricity is carried out by water electrolysis, which produces H₂. The consumption of this H₂ together with CO₂ (or CO), through the Sabatier reaction (Equation (1) or Equation (2)), produces methane, water, and heat [6].



When the electrolyser is fed from a renewable energy source, the obtained synthetic natural gas (SNG) can be considered neutral in CO₂ emissions. The amount of CO₂ that is emitted by this SNG is the same as that is required for its own formation [7]. To make the most of this technology, one can use it with oxy-fuel combustion, since it produces a

pure stream of CO₂ for the methanation, while electrolysis provides pure O₂ for the oxy-fuel combustion [7–10].

In the case of the iron and steel industry, electrolysis can be performed as usual on water to produce H₂ or on the CO₂ emissions of the industry to obtain syngas (CO₂ electrolysis). Both the syngas and the H₂ produced can be used in a methanation process to obtain methane (power-to-methane) [11].

Power-to-H₂ can be integrated in ironmaking in two ways. The first method consists in injecting the H₂ as auxiliary reducing agent in conventional BFs to reduce the carbon content of the fossil reducing gas, while the second technique uses the H₂ as reducing agent in DRI reactors. Studies assessing the injection of H₂ in BFs show the potential of reducing CO₂ emissions by approximately 20%, barely affecting the overall energy demand of the process. In this case, the injected flow of H₂ should be around 30 kg H₂/t pig iron, to not significantly modify the operating conditions inside the furnace. Regarding the second method, i.e., DRI, integration of power-to-H₂ has the potential to lead to the low energy consumption (3.5–3.7 MWh/t steel) and net-zero CO₂ emissions (if carbon-free electricity is used, corresponding to 97–100% emission reduction). Still, to make the power-to-H₂-DRI route competitive, carbon allowances should reach approximately EUR 62 per t CO₂ and electricity price should be below EUR 40 per MWh_e [11]. The subsequent process following the DRI, i.e., the EAF, can also benefit from power-to-methane integrations, as partial substitution of electrical energy by natural gas in EAF may be beneficial for CO₂ reduction, thanks to the increment in the efficiency of the process [12].

Since 95% of the world's iron production is coal-based, it is important to focus on the BF-BOF route, which is the focus of this study. Power-to-syngas and power-to-methane can supply a useful fuel to be injected in a conventional BF, acting as a renewable reducing agent (recycled CO₂) [11]. Recent studies have concluded that CO₂ emission reduction in power-to-syngas, compared to conventional ironmaking, could be in the range of 11% to 22%, with typical electrolysis capacities of 100–900 MW. In the case of power-to-methane, the CO₂ reduction would be between 13% and 19%, requiring water electrolysis power capacities of about 880 MW [11,13].

The objective of this paper was to study a novel concept that integrates power-to-gas technology in the iron and steel industry, together with oxy-fuel combustion and top gas recycling. Two types of integration, which differ in the source of the H₂ (water electrolysis or COG), were studied and compared to a reference iron and steel plant in terms of energy requirement and emission reduction. The main novelty of the study relied on the reduction of energy penalties thanks to the combination of power-to-gas and oxy-fuel combustion, which has not been quantified so far in the literature specifically for the iron and steel industry.

2. Description of Case Studies

Three case studies were undertaken to evaluate the energy requirements and carbon emission reductions of power-to-gas (PtG) integrated with blast furnace-basic oxygen furnace (BF-BOF) plants relative to a conventional reference BF-BOF process. The reference plant is described in Section 2.1. The proposed power-to-methane integration in ironmaking with oxy-fuel combustion and top gas recycling (TGR) is described in Section 2.2, and methanation of coke oven gas (COG) integration in ironmaking with oxy-fuel combustion and TGR in Section 2.3.

2.1. Case 0: Reference Plant for BF-BOF Ironmaking

The plant consists of a sintering process, coke oven, hot stoves, BF, air separation unit (ASU), BOF, and casting and rolling. The block diagram of the reference ironmaking plant is shown in Figure 2, for which an average production of 2.8 million t_{steel}/year (7.7 kt/day) was assumed [14]. For the sake of simplicity, secondary processes were neglected (e.g., material recirculation in sintering), such as in similar studies [15,16]. The rele-

vance of these processes to this study is minor since the objective was to conduct a first assessment of the novel integration under overall energy and mass balances.

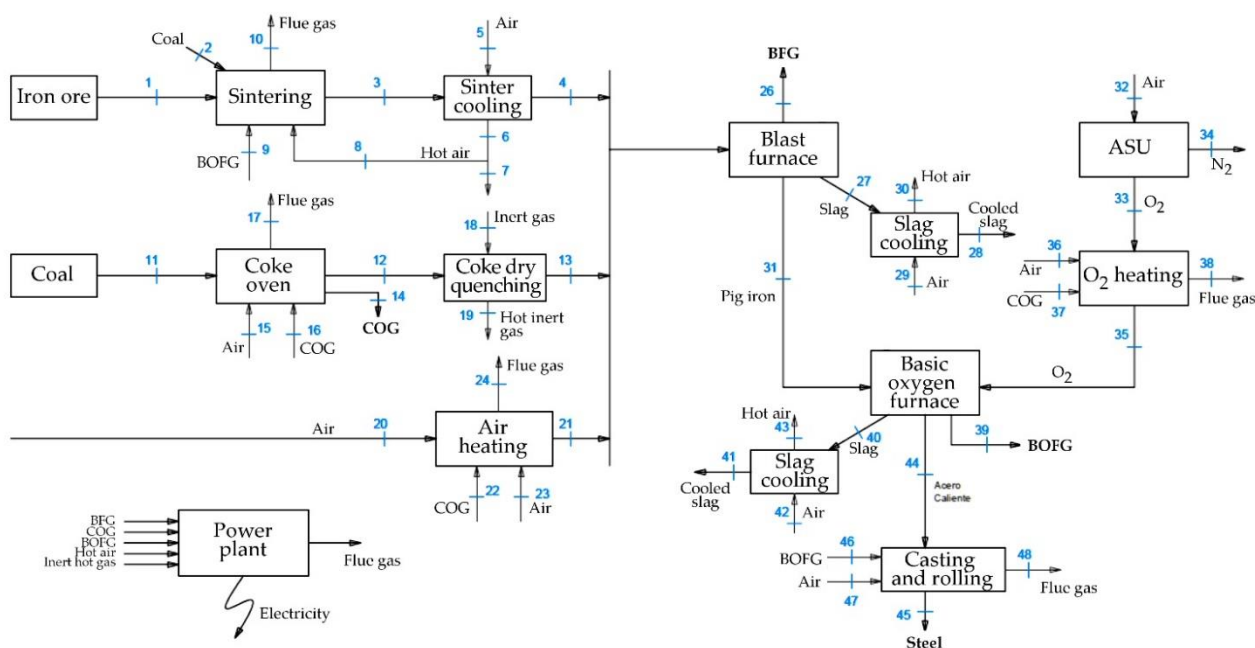


Figure 2. Block diagram of the reference ironmaking plant (Case 0).

The main input mass flows were iron ore, coal (converted to pure C in the coke oven), and air (for combustion in BF and for oxygen production in the ASU), as shown in Figure 2. Regarding the inputs to the BOF, we assumed that only pig iron was used (without scrap metal), as in others studies [3,4,15,16]. Those processes requiring heat at high temperature were supplied with thermal energy by consuming part of the fuel gases by-produced in the coke oven, BF and BOF (Table 1) instead of using additional fossil fuels.

In addition, there was a power plant for the utilization of the remaining COG, BFG, and BOFG, as well as for gas streams at high temperature coming from cooling processes (sinter, slag, and coke cooling).

Table 1. Elemental composition of the fuel gases produced as by-products in the ironmaking plant (vol %) [3].

	Natural Gas	COG	BFG	BOFG
H ₂	0	56	4	1.5
CH ₄	100	30	0	0
CO	0	10	25	66.5
CO ₂	0	5	20	20
O ₂	0	1	0	2
N ₂	0	5	51	10

2.2. Case 1: Power-to-Methane Integration in Ironmaking with Oxy-Fuel Combustion and TGR

The modified ironmaking plant integrated with power-to-methane in Case Study 1 is depicted in Figure 3. The BF was here operated under oxy-fuel regime, and coke input to the BF was partially replaced by synthetic methane (stream 140, Figure 3). Part of the blast furnace gas (BFG) (stream 157) was recirculated (top gas recycling (TGR)), and the other was diverted to the power-to-gas plant (stream 157). Here, the emissions of the BF were used to obtain synthetic methane again by combining them with the H₂ from a low temperature electrolyser (stream 182). Thus, a continuous recycling of CO₂ was established. Moreover, the O₂ from the electrolyser (stream 183) was used for the oxy-fuel

combustion in the BF, which allowed us to significantly reduce the ASU energy consumption. In addition to the above new equipment necessary for the power-to-gas integration, new preheating blocks (O₂ + BFG preheating and CH₄ preheating) were also included.

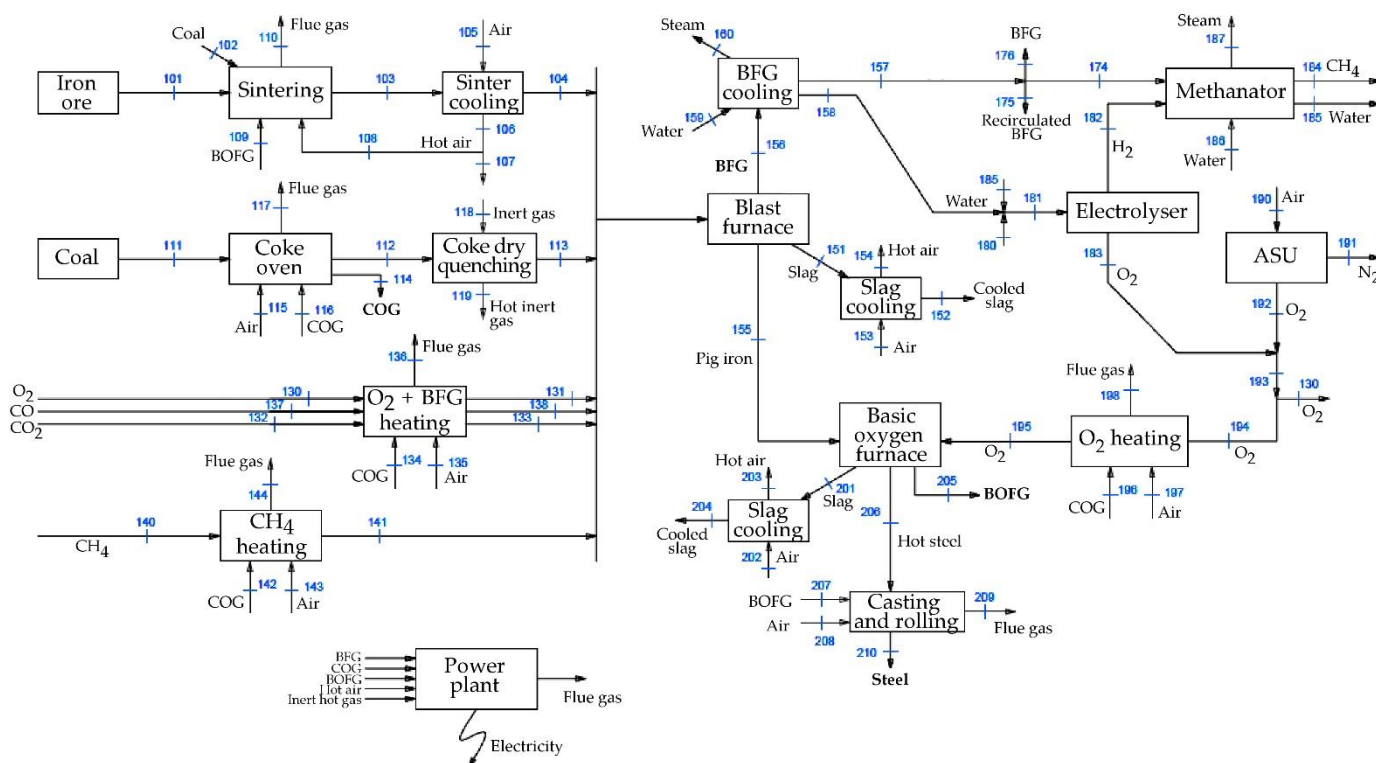


Figure 3. Block diagram of the integration of power-to-methane in ironmaking with oxy-fuel combustion and TGR (Case 1).

The oxy-blast furnace chosen for this case study ran in a nitrogen-free atmosphere. A pure stream of oxygen was introduced through the tuyeres instead of hot air, in order to obtain exhaust gases that were also nitrogen-free (composed only of CO₂ and CO). This concept is closely related to the top gas recycling. The TGR technology consists of recirculating the exhaust gases (mainly CO₂, CO, and H₂) back to the BF to reduce the coke (and consequently the air) consumption, which made the final BFG contain less N₂. In the present case, both oxyfuel and TGR technologies were simultaneously applied. The reason for applying TGR was that introducing a reducing gas (CO) diminished the coke consumption, while separating CO and CO₂ would have an energy penalization. The selected proportion between O₂ and CO₂ in the oxy-blast furnace was 40% O₂–60% CO₂.

The gas introduced in the methanation reactor was BFG, since it contains no nitrogen and large proportions of CO, which reduced the methanator H₂ requirement.

2.3. Case 2: Methanation of COG Integration in Ironmaking with Oxy-Fuel Combustion and TGR

The modified ironmaking plant for power-to-methane integration for Case Study 2 is depicted in Figure 4. In this case, the ironmaking worked in the same oxy-fuel regime with TFG as in Case 1, but here the COG (stream 114/382) was used as H₂ source in the methanation process instead of pure H₂. Since COG does not contain nitrogen, and has large contents of CH₄, H₂, and CO, it completely avoided the need for an electrolyser and its associated investment cost, unlike in Case 1. The rest of the operating conditions and assumptions remained the same as in the Case Study 1.

In summary, in terms of produced gas utilization, Case 1 recycled BFG to the methanator and SNG to the BF, while Case 2 recycled both BFG and COG to the methanator and SNG to the BF.

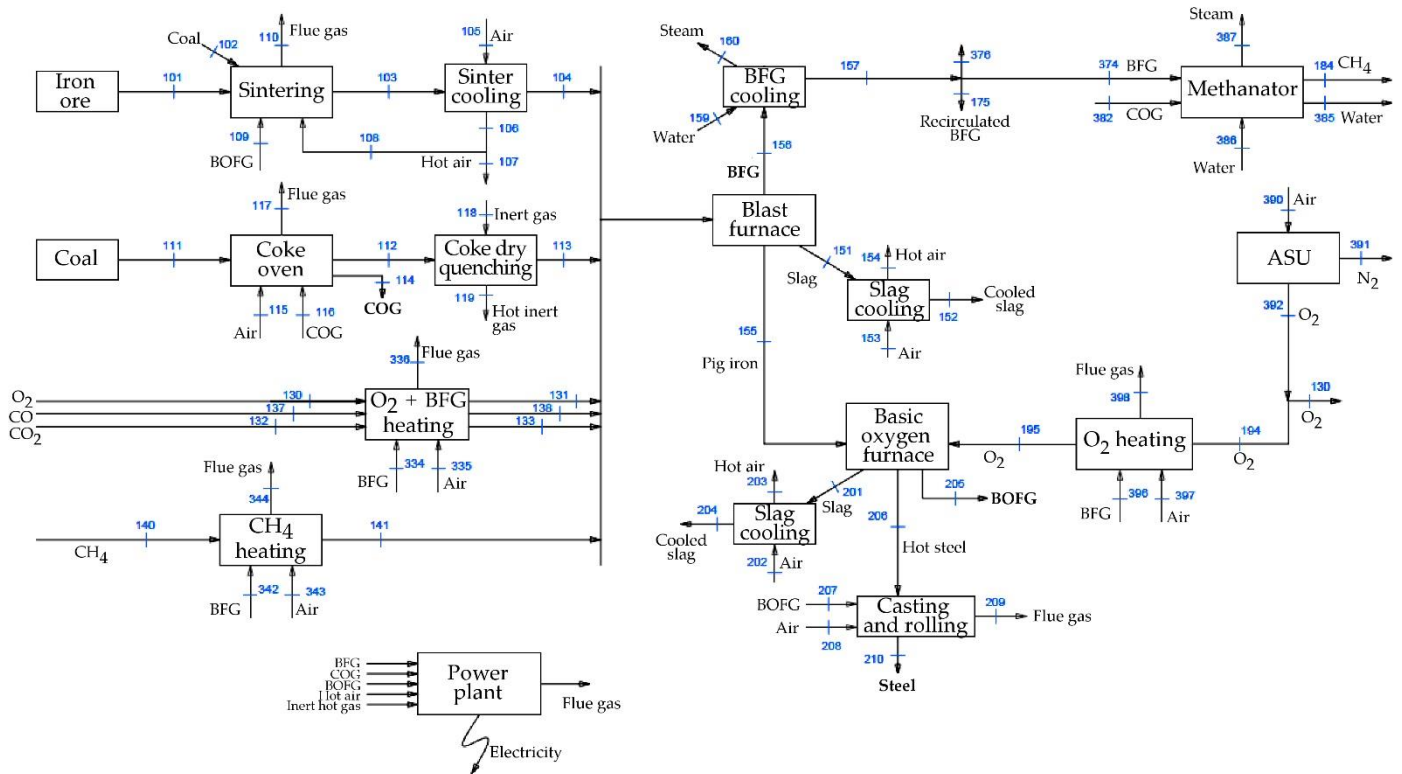


Figure 4. Block diagram of the integration of COG methanation in ironmaking with oxy-fuel combustion and TGR (Case 2).

3. Methodology

The modelling assumptions common to the analyses of Cases 0–2 plant concepts included steady-state conditions, ideal gases, and adiabatic reactions. Further case-specific assumptions are documented in Section 3.1.

The modelling methodology is based on overall mass balance (Equation (3)) and energy balance (Equation (4)) in steady state, applied to each equipment in Case 0, Case 1, and Case 2 plant layouts (Figures 2–4).

$$0 = \sum m_i - \sum m_o \quad (3)$$

$$0 = Q - W + \sum m_i h_i - \sum m_o h_o \quad (4)$$

where m is the mass flow, h the specific enthalpy, W the network, and Q the net heat transfer. Enthalpy can be written as Equation (5), where $\Delta_f h_i^{T_{ref}}$ is the enthalpy of formation at the reference temperature and c_p is the temperature-dependent specific heat.

$$h_i = \Delta_f h_i^{T_{ref}} + \int_{T_{ref}}^T c_{p,i} dT \quad (5)$$

When necessary, data from the literature were used. The specific assumptions for the subsystems (ironmaking, power plant, and power-to-gas) are described in the following subsections.

3.1. Iron and Steel Plant

For Case 0, in the ironmaking process (BF), instead of fixing the input mass flows of iron ore (Stream 1, Figure 2), coal (Stream 11, Figure 2), and hot blast (Stream 20, Figure 2), we calculated them from the mass balance by assuming a final composition of the steel and the BFG, taken from [17] and [3], respectively. The mass fraction of iron was set at 96% in pig iron and 99.7% in steel, with carbon as the remaining component (other elements such as Si or Mn were neglected) [17]. The mole fraction of the BFG was fixed according to data from [3] in Table 1. The mass flows of the pig iron (Stream 31, Figure 2), BFG (Stream 26, Figure 2), and slag (Stream 27, Figure 2) were also calculated in the BF's mass and energy balances. The air for the hot blast was heated to 1200 °C by means of COG (Stream 22, Figure 2) [18].

The coal added to the sintering process was set at 5 wt % of the amount of iron treated [19]. The temperature of the sintered iron at the exit of this sintering process was assumed at 800 °C (Stream 3, Figure 2), which was later reduced to 150 °C (Stream 4, Figure 2) [16]. The amount of BOFG (Stream 9, Figure 2) and the cooling air (Stream 5, Figure 2) were calculated with the mass and energy balances for each block.

The coke produced in the coke oven was assumed as pure carbon, and the mole fraction of the COG was fixed as shown in Table 1. The coke temperatures before and after the coke dry quenching (CDQ) were 1100 °C (Stream 13, Figure 2) and 150 °C (Stream 13, Figure 2), respectively [2]. The mass flow of COG was calculated in a mass balance between the input coal and the output coke. The self-consumed COG and the inert gas needed for the CDQ were calculated in mass and energy balances for each block.

Regarding the air separation unit required for the BOF, we assumed that it produced pure streams of O₂ (Stream 33, Figure 2) and N₂ (Stream 34, Figure 2). The electricity consumption of the ASU was set at 1440 kJ per kilogram of oxygen produced [20]. The pure stream of oxygen was heated up to 1650 °C [3] by burning COG (Stream 37, Figure 2).

In the BOF, the amount of hot steel produced was assumed as a unit reference (1 kg of steel). The composition of the BOFG was again fixed according to Table 1, and the mass flows of slags (Stream 40, Figure 2), BOFG (Stream 39, Figure 2), and O₂ (Stream 35, Figure 2) were calculated by a mass and energy balance in the BOF.

For Cases 1 and 2, the assumptions and methodology explained for Case 0 were the same, with some minor changes. In the BF's mass balance, not only the iron ore, coal, BFG, and pig iron mass flows were calculated, but also the O₂ (Stream 130, Figure 3), CH₄ (Stream 140, Figure 3), and BFG (recirculated) (Stream 175, Figure 3). The O₂ demand for the BOF remained the same (Stream 195, Figure 2), but the amount of O₂ produced by the ASU was lower (Stream 192, Figure 2), since a by-product stream of O₂ from the electrolyser was used (Stream 183, Figure 3) (only for Case 1).

3.2. Power Plant

This plant produces electricity for self-consumption from the energetic gases of the steel plant (i.e., COG, BFG, BOFG) and from heat streams from other heat recovery processes (i.e., coke dry quenching and slag cooling). An overall efficiency of 17.9% was assumed for the power plant [16], because of the low temperatures of the heat recovery flows, the gas treatment before entering the boiler, and the limited calorific value of the gases (due to the high CO₂ content and the dilution in the N₂ present in the air).

3.3. Power-to-Gas Plant

In Case Study 1, the H₂ was produced from water electrolysis, while in Case Study 2, the H₂ came from the COG, which was directly diverted to methanation. The COG contained enough H₂ to produce all the necessary methane, but lacked CO₂. Therefore, some BFG was also diverted to methanation to fulfil the stoichiometric requirements of reactions (1) and (2). It is important to note that in Case 2, no electrolyser was needed. The methanation plant worked at 300 °C and 30 bar [7].

For the sake of simplicity, the electrolyser was assumed to produce pure streams of O₂ and H₂, while the methanation was set to produce a pure stream of methane. By these assumptions, as well as reactions (1) and (2), we can easily solve the mass balance. Regarding electricity, the energy consumption of the low-temperature electrolyser was fixed at 4.5 kWh/Nm³ [7,8,21].

4. Results and Discussion

The modelling results obtained for Cases 0, 1, and 2 are presented and discussed in Sections 4.1–4.3, respectively. In addition, the corresponding stream data for each Case are presented in the Appendix A.

4.1. Case 0: Reference Plant for BF-BOF Ironmaking

The mass flows of Case 0 are summarized in Table 2, where the main calculated variables are compared to data from the literature [3,11,15–17]. All results lay within reasonable limits, thus validating the results of the reference case, which was the basis for the rest of the analyses. As already stated in the methodology section, the input streams were calculated as a function of a desired steel output composition.

The total electricity consumption of the ironmaking process was 874 MJ/t steel, and the electricity produced by the power plant was 1260 MJ/t steel (Table 3); therefore, the overall process was self-sufficient (typical power productions were about 1300 MJ/t steel in on-site power plants [15]). Regarding the thermal energy consumption, the BF was the largest consumer, representing 55% of the overall process when the air heating was accounted for (in the literature, the energy consumption of the blast furnace (BF) process can reach 70% of the total plant [3]). The heat removed by cooling the stoves of the BF was fixed at 1260 MJ/t pig iron, according to [22].

Table 2. Mass flows (kg/t steel) of the main streams calculated for Case 0, Case 1, and Case 2. Bibliography data were taken from [3,11,15–17]. * Note: input data for solving mass and energy balances.

	Stream	Bibl.	Case 0	Case 1	Case 2
Raw materials	Iron ore	1550	1430	1430	1430
	Coal	560	520	460	460
Coke oven	COG	90	110	90	90
	Sinter	1550	1430	1430	1430
	Coke	400	420	370	370
	Air (hot blast)	1210	1280	-	-
Blast furnace (BF)	O ₂ (hot blast)	-	-	310	310
	BFG (hot blast)	-	-	1060	1060
	CH ₄ (hot blast)	-	-	65	65
	BFG	2420	2080	2190	2190
	Slag	280 *	280	280	280
	Pig iron	1040 *	1040	1040	1040
	O ₂	70	90	90	90
Basic oxygen furnace (BOF)	Steel	1000	1000	1000	1000
	Slag	80 *	80	80	80
	BOFG	130 *	130	130	130
	O ₂	-	-	210	-
Power-to-gas (PtG)	H ₂	-	-	27	-
	BFG	-	-	139	14
	COG	-	-	-	91
	CH ₄	-	-	65	65

Table 3. Main energy streams (MJ/t steel) calculated for Case 0, Case 1, and Case 2. * From: [15].

Process		Case 0	Case 1	Case 2
Thermal energy consumption	Sintering	523	523	523
	Coke oven	1631	1442	1442
	Air (hot blast)	1814	-	-
	O ₂ + BFG (hot blast)	-	1239	1239
	CH ₄ (hot blast)	-	431	431
	Blast furnace	2915	3900	3900
	O ₂ heating	170	170	170
	BOF	1228	1228	1228
	Casting, rolling	300	300	300
	Total	8581	9233	9233
Electricity consumption	Sintering *	180	180	180
	Coke oven *	42	42	42
	Blast furnace *	376	376	376
	ASU	128	252	568
	BOF *	128	128	128
	Electrolyser	-	4991	-
	H ₂ compressor	-	96	32
	CO ₂ compressor	-	51	36
	Other *	20	20	20
	Total	874	6136	1382
Electricity production	Power plant	1260	1443	652

The percentage of utilization of COG, BFG, and BOFG by type of process is presented in Table 4, together with their energy density and mass flow production. In overall terms, the 46.5% energy content of these gases was used in internal processes of the plant, while the rest was used in the power plant (Figure 5). The total CO₂ emissions of the plant were 1718 kg/t steel (Figure 6), with BFG as the major emitting source (1368 kg/t steel). According to the literature, BF CO₂ emissions may range between 1270 and 1550 kg/t steel, and total emissions up to 2200 kg/t steel [16,23].

Table 4. Mass flow, energy content, and use of the fuel gases produced in the ironmaking process.

		Case 0			Case 1			Case 2		
		COG	BFG	BOFG	COG	BFG	BOFG	COG	BFG	BOFG
Utilization of the energy content of the gases by type of process (%)	Mass flow (kg/t steel)	110	2080	130	90	2140	130	90	2140	130
	Energy content (MJ/kg)	40.0	2.7	6.3	40.0	5.7	6.3	40.0	5.7	6.3
	Internal use	99.1	0	99.0	0	42.2	99.0	0	43.6	99.0
	Power plant	0.9	100	1.0	100	1.6	1.0	0.3	6.0	1.0
	Methanation	-	-	-	0	6.5	0	99.7	0.6	0
	TGR	-	-	-	0	49.7	0	0	49.7	0

4.2. Case 1: Power-to-Methane Integration in Ironmaking with Oxy-Fuel Combustion and TGR

In Case 1, the installation included an oxygen blast furnace with top gas recycling and a power-to-gas (PtG) plant. The latter converted the CO₂ emissions into synthetic methane to be reinjected in the blast furnace, thus replacing some fossil fuel. The power capacity of the power-to-gas plant was sized to produce a SNG amount enough to replace 50 kg coke/t steel. According to the simulation, the replacement ratio was 1.3 kg SNG/kg coke, and therefore the necessary H₂ was 27 kg H₂/t steel. Assuming a steel production of 7.7 kt/day, we found the electrolysis power capacity to be installed was 431.9 MWe if working continuously (4.5 kWh/Nm³ H₂ electricity consumption). Currently, the world's largest planned electrolyser farm has a power capacity of 100 MW [24], which is

within the same order of magnitude as the PtG capacity required for the proposed case study.

The total electricity consumption of the overall plant was 6.1 MJ/t steel, which means an increment of 702% with respect to the base case scenario (Table 3). The electricity demand of those processes already existing in the base simulation was kept constant [15], and the new electricity consumptions corresponding to the PtG plant were added (the production of H₂ represents 81% of the total electricity consumption). Despite the power plant now producing 14.5% more power (1.4 MJ/t steel), the overall process is no longer self-sufficient. The remaining electricity (4.7 MJ/t steel) should come from renewable sources to avoid further emissions. Within this framework, a renewable facility working continuously of 417 MW_e is required to satisfy this electricity demand.

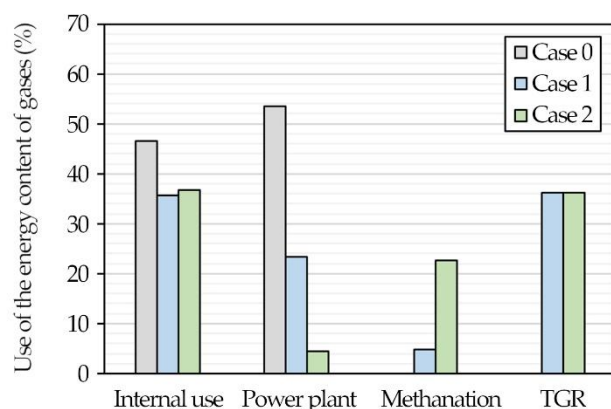


Figure 5. Use of the energy content of the total gases (COG, BFG, and BOFG) by type of process for each plant layout (i.e., Case 0–2).

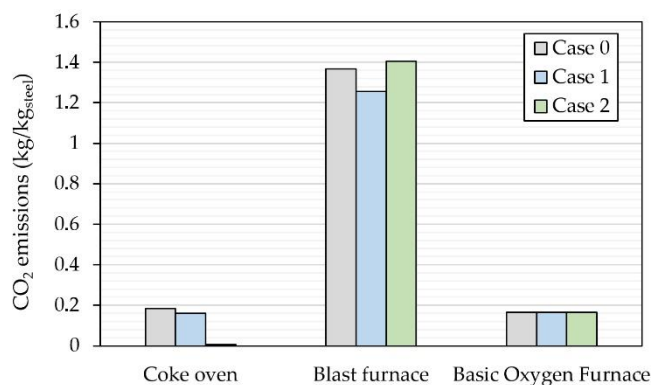


Figure 6. CO₂ emissions by process for each plant layout (i.e., Case 0–2).

Regarding thermal energy consumption (Table 3), the largest consumer is still the blast furnace (60.3% of the total needs). Its energy consumption increased by 9.4% due to oxy-fuel combustion. However, the coke oven consumption decreased by 11.6% due to the reduction of fossil fuel input. In the air heating furnace, we had to heat CO₂ for the oxy-combustion instead of air, resulting in a slight reduction of the thermal energy consumption.

In this integration, BFG was used in top gas recycling and methanation, and therefore the percentage of utilization of fuel gases by type of process remarkably changed (Table 4). Here, only 35.7% of the energy content of these gases was used in the internal processes of ironmaking and 21.4% in the power plant (Figure 5). The remaining was mostly recirculated to the blast furnace (36.1%), and a small fraction was diverted to methanation (4.7%).

Regarding CO₂, the BF was still the larger emitting source, producing 1255 kg/t steel. In total, the CO₂ emissions were 1582 kg/t steel, which was 8% less than in the ref-

erence case (Case 0, Figure 6). Thus, 136 kg CO₂/t steel were avoided by consuming 5079 MJ/t steel additional electrical energy, and a saving of 3.34 MJ/kg CO₂ by means of coke reduction was achieved, which means a CO₂ avoidance penalization of 34 MJ/kg CO₂. Comparing this penalization with those in other processes, such as power-to-syngas (4.8–10.8 MJ/kg CO₂ [11]) and amine scrubbing (3–4 MJ/kg CO₂ [25,26]), indicates that Case 1 configuration does not present any energy advantage.

4.3. Case 2: Methanation of COG Integration in Ironmaking with Oxy-Fuel Combustion and TGR

In this case, the ironmaking process worked under oxy-fuel regime with top gas recycling as in Case 1. However, here, the H₂ source for the methanation process was the coke oven gas instead of pure H₂.

The total electrical consumption of this plant was 1382 MJ/t steel. This was well below Case 1 (77% lower) since electrolysis was no longer used, but still above Case 0 (58% higher) because of the gas compression in the methanation process and the production of O₂ for the oxy-fuel blast furnace. Moreover, since COG was here used in methanation, the power plant only produced 652 MJ/t steel (47% of the total electricity consumption, i.e., not self-sufficient). To supply the missing electricity, we required a renewable facility of 65 MW_e working continuously, assuming a steel production of 7.7 kt/day. Regarding thermal energy consumption, the requirements are the same than those of Case 1 (Table 3).

In terms of gas utilization (Table 4), the COG was used entirely in methanation instead of in internal plant processes. For this reason, 43.6% of the BFG had to be allocated to this end. The BOFG was also used in the internal processes of the plant (as in the two previous cases). With this implementation, 36.8% of the energy from these gases was used in the internal processes, 4.5% in the power plant, 22.6% in methanation, and 36.1% in top gas recycling (Figure 5).

Regarding emissions, the CO₂ that was avoided remained the same as for Case 1 (136 kg CO₂/t steel) because the same amount of methane was produced, and therefore the amount of CO₂ that was recycled in closed loop did not change. Then, total emissions were 1582 kg/t steel (the BF accounted for 1405 kg CO₂/t steel, while the coke oven barely emitted CO₂ because COG was used in methanation). Since the electricity consumption increased by 1116 MJ/t steel, the CO₂ avoidance penalization was 4.9 MJ/kg CO₂. This penalization is in the range of other processes such as power-to-syngas or amine scrubbing, and therefore is energetically competitive.

4.4. Discussion

Figure 7 depicts a Sankey diagram of the energetic gases of the steel industry for the three scenarios: Case 0, Case 1, and Case 2. It can be seen that the energy flow to the power plant was increasingly reduced for each case, thus explaining why a renewable facility is needed. The internal energy use increased in Cases 1 and 2 due to the blocks that were added to the diagram (e.g., CH₄ heating). In the methanation section, the same energy was consumed in both Cases 1 and 2, and therefore the main difference was the H₂ source, either an electrolyser or the COG. The TGR was not changed in the two integrations, obtaining the energy from the BFG.

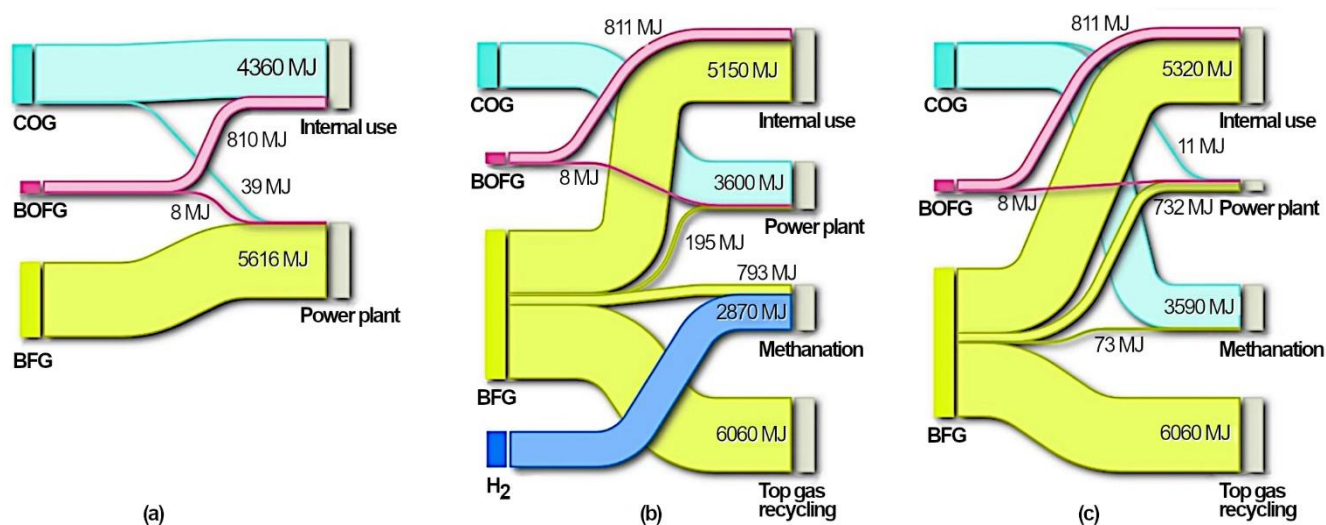


Figure 7. Sankey diagram of the change in the energy utilization inside the ironmaking plant of the energetic gases COG, BOFG, and BFG: (a) Case 0, (b) Case 1, and (c) Case 2.

Although integrating oxy-fuel combustion in the BF is an interesting option in terms of CO₂ mitigation, the technology is not commercial yet (current TRL is 6–7) [27]. Thus far, Zuo and Hirsch [28] reported experimental results from a 9 m³ TGR-BF, combined with a vacuum pressure swing adsorption carbon capture method for removing CO₂ of the top gas. They found 24% savings in carbon consumption and 76% reduction in CO₂ emissions when assuming underground storage of the corresponding captured CO₂ [29]. On average, the carbon input decreased from 470 kg/t pig iron to 350 kg/t pig iron [27]. It is worth mentioning that oxy-fuel combustion is already applied commercially in secondary processes in ironmaking plants, such as during the preheating of ladles and converter, or during the steel reheating and heat treatment. Since the oxy-fuel technology is familiar to the industry, its adoption in BFs is a reasonable option [11]. In fact, the topic is being studied widely in the literature to solve remaining technical issues related to the smoothness of operation (non-linear behavior of the feedback induced by the top gas recycle) [30].

5. Conclusions

A novel concept integrating power-to-gas technology in the ironmaking process, together with oxy-fuel combustion and top gas recycling, was presented. Two integration options were analyzed, differing in the source of H₂ for the methanation process (H₂ from water electrolysis, Case 1, or syngas from the coke oven, Case 2). In both cases, synthetic natural gas from methanation was injected into the blast furnace to reduce the coke consumption, thus recycling CO₂ in a closed loop. The power-to-gas plant was sized to reduce the coke content by 50 kg/t steel. Both Cases 1 and 2 were compared with a conventional ironmaking process (Case 0).

The base case simulation included the sintering process, coke oven, hot stoves, blast furnace, air separation unit, basic oxygen furnace, casting, and power plant. For the power-to-gas (PtG) integrations, an electrolyser (only in Case 1) and methanation plant were added to the simulation, and the blast furnace was run under oxy-fuel conditions with top gas recycling. Mass flows, compositions, and thermal and electricity consumptions were calculated through mass and energy balances.

Savings in CO₂ emissions with either of the two PtG implementations were 8%, with a reduction in coal fuel of 12.8%. The energy required to avoid these emissions was 34 MJ/kg CO₂ for Case 1 and 4.9 MJ/kg CO₂ for Case 2. This remarkable difference was because the first PtG integration required a 431.9 MW electrolyser to produce the H₂,

while the second used the H₂ content of coke oven gas (COG) and therefore an electrolyser was not needed. Under this framework, the only competitive option is Case 2, whose energy penalization is in the range of conventional amine carbon capture [31]. Moreover, it has the advantage of reducing the fuel consumption and reducing geological storage, which are additional benefits regarding economic costs compared to conventional carbon capture and storage.

The energy content of the gases generated in the industry (COG, BFG, and BOFG) are normally used in internal processes, but mainly in the production of electricity. The implementation of the PtG implies a greater consumption of these gases in the internal processes of the plant, as well as in the methanation and recirculation processes. This means that only a small percentage of the gases are diverted to the thermal power plant, making necessary a renewable facility to fulfil the electricity demand (in Case 1 and Case 2, the plant is no longer self-sufficient). Case 1 requires a renewable-based power production 5.2 times larger than Case 2 (417 MW vs 65 MW), due to electrolysis.

This study shows good technical prospects for the future in terms of reducing steelmaking industry emissions. An economic analysis of the proposed alternative processes will be performed in future work.

Author Contributions: Conceptualization, J.P., M.B., L.M.R., and B.P.; methodology, J.P. and M.B.; model, J.P. and M.B.; validation, J.P. and M.B.; formal analysis, J.P.; writing—original draft preparation, J.P. and M.B.; writing—review and editing, V.E.; visualization, J.P. and M.B.; supervision, M.B., L.M.R., B.P., and V.E.; project administration, M.B., L.M.R., B.P., and V.E.; funding acquisition, M.B., L.M.R., and V.E. All authors have read and agreed to the published version of the manuscript.

Funding: The work described in this paper has been supported by both the University of Zaragoza under the project UZ2020-TEC-06 and Khalifa University project CIRA-2020-080. This work has also received funding from the European Union’s Horizon 2020 research and innovation program under the Marie Skłodowska-Curie grant agreement no. 887077.

Institutional Review Board Statement: Not applicable.

Informed Consent Statement: Not applicable.

Data Availability Statement: Data included in the paper.

Conflicts of Interest: The authors declare no conflict of interest.

Abbreviations

ASU	air separation unit
BAT	best available technology
BF	blast furnace
BFG	blast furnace gas
BOF	basic oxygen furnace
BOFG	basic oxygen furnace gas
CDQ	coke dry quenching
CO	coke oven
COG	coke oven gas
PtG	power-to-gas
SNG	synthetic natural gas
TGR	top gas recycling

Appendix A – Stream data

Table A1. Specific heat, mass flows, and temperatures for Cases 0, 1 and 2.

Stream	cp	m	T	Stream	cp	m	T	Stream	cp	m	T
	(kJ/kg.K)	(kg/kgsteel)	(°C)		(kJ/kg.K)	(kg/kgsteel)	(°C)		(kJ/kg.K)	(kg/kgsteel)	(°C)
1	0.473	1.426	25	49	0.907	0.085	25	180	4.18	0.08955	25
2	0.835	0.0713	25	101	0.473	1.426	25	181	4.18	0.2414	25
3	0.473	1.426	800	102	0.835	0.0713	25	182	14.34	0.02701	25
4	0.473	1.426	150	103	0.473	1.426	800	183	0.914	0.2144	25
5	1.005	0.6232	25	104	0.473	1.426	150	184	2.239	0.06506	25
6	1.126	0.6232	650	105	1.005	0.6232	25	185	4.18	0.1016	25
7	1.126	0.4762	650	106	1.126	0.6232	650	186	4.18	2.665	25
8	1.126	0.147	650	107	1.126	0.4762	650	187	4.18	2.665	80
9	1.426	0.08527	25	108	1.126	0.147	650	190	1.005	0.7772	25
10	1.012	0.2374	500	109	1.426	0.08527	25	191	1.038	0.5938	25
11	0.835	0.5238	25	110	1.012	0.2374	500	192	0.914	0.1803	25
12	0.836	0.4191	1100	111	0.835	0.4568	25	193	0.914	0.3947	25
13	0.836	0.4191	150	112	0.836	0.3654	1100	194	0.914	0.08873	25
14	9.035	0.1048	1350	113	0.836	0.3654	150	195	1.179	0.08873	1650
15	1.005	0.668	25	114	9.035	0.09136	1350	196	1.117	0.04026	25
16	9.035	0.04969	25	115	1.005	0.4562	25	197	1.005	0.05914	25
17	1.012	0.7408	500	116	1.117	0.3105	25	198	1.012	0.104	600
18	1.038	0.3646	25	117	1.012	0.8021	500	200	0.907	0.085	25
19	1.178	0.3646	800	118	1.038	0.318	25	201	0.749	0.085	1650
20	1.005	1.278	25	119	1.178	0.318	800	202	1.005	0.06183	25
21	1.208	1.278	1200	130	0.914	0.3059	25	203	1.154	0.06183	800
22	9.035	0.05062	25	131	1.142	0.3059	1200	204	0.749	0.085	460
23	1.005	0.6805	25	132	0.842	0.5324	25	205	1.426	0.1346	1650
24	1.012	0.7547	300	133	1.323	0.5324	1200	206	0.5	1	1650
25	0.907	0.283	25	134	1.117	0.4782	25	207	1.412	0.04795	25
26	1.412	2.084	200	135	1.005	0.7025	25	208	1.005	0.08269	25
27	0.749	0.283	1200	136	1.012	1.235	600	209	1.012	0.1335	850
28	0.749	0.283	460	137	1.037	0.53	25	210	0.5	1	25
29	1.005	0.1754	25	138	1.254	0.53	1200	334	1.412	0.4782	25
30	1.154	0.1754	800	140	2.239	0.06506	25	335	1.005	0.7025	25
31	0.48	1.039	1200	141	5.632	0.06506	1200	336	1.012	1.235	600
32	1.005	0.3825	25	142	1.117	0.1019	25	342	1.412	0.1019	25
33	0.914	0.08873	25	143	1.005	0.1498	25	343	1.005	0.1498	25
34	1.038	0.2922	25	144	1.012	0.2633	600	344	1.012	0.2633	600
35	1.179	0.08873	1650	150	0.907	0.283	25	374	1.412	0.01384	25
36	1.005	0.07301	25	151	0.749	0.283	1200	376	1.098	1.059	25
37	9.035	0.00543	25	152	0.749	0.283	460	382	9.035	0.09106	25
38	1.012	0.08096	600	153	1.005	0.1754	25	385	4.18	0.00883	25
39	1.426	0.1346	1650	154	1.154	0.1754	800	386	4.18	0.8714	25
40	0.749	0.085	1650	155	0.48	1.039	1200	387	4.18	0.8714	80
41	0.749	0.085	460	156	1.117	2.186	200	390	1.005	1.701	25
42	1.005	0.0847	25	157	1.098	2.136	25	391	1.038	1.3	25
43	1.154	0.0847	800	158	4.18	0.05031	25	392	0.914	0.3947	25
44	0.5	1	1650	159	4.18	2.352	25	396	1.412	0.04026	25
45	0.5	1	25	160	4.18	2.352	80	397	1.005	0.05914	25
46	1.426	0.04795	25	174	1.098	0.1389	25	398	1.012	0.104	600
47	1.005	0.08269	25	175	1.098	1.062	25				
48	1.012	0.1335	850	176	1.098	0.9343	25				

References

1. Huitu, K.; Helle, H.; Helle, M.; Kekkonen, M.; Saxén, H. Optimization of steelmaking using fastmet direct reduced iron in the blast furnace. *ISIJ Int.* **2013**, *53*, 2038–2046. <https://doi.org/10.2355/isijinternational.53.2038>.
2. Quader, M.A.; Ahmed, S.; Ghazilla, R.A.R.; Ahmed, S.; Dahari, M. A comprehensive review on energy efficient CO₂ breakthrough technologies for sustainable green iron and steel manufacturing. *Renew. Sustain. Energy Rev.* **2015**, *50*, 594–614. <https://doi.org/10.1016/j.rser.2015.05.026>.
3. He, K.; Wang, L. A review of energy use and energy-efficient technologies for the iron and steel industry. *Renew. Sustain. Energy Rev.* **2017**, *70*, 1022–1039. <https://doi.org/10.1016/j.rser.2016.12.007>.
4. Ariyama, T.; Takahashi, K.; Kawashiri, Y.; Nouchi, T. Diversification of the Ironmaking Process Toward the Long-Term Global Goal for Carbon Dioxide Mitigation. *J. Sustain. Metall.* **2019**, *5*, 276–294. <https://doi.org/10.1007/s40831-019-00219-9>.
5. Lisbona, P.; Bailera, M.; Peña, B.; Romeo, L.M. Integration of CO₂ capture and conversion. In *Advances in Carbon Capture*; Rahimpour, M.R., Farsi, M., Makarem, M.A., Eds.; Woodhead Publishing, Cambridge, United Kingdom: 2020; pp. 503–522, ISBN 9780128196571.
6. Gao, J.; Wang, Y.; Ping, Y.; Hu, D.; Xu, G.; Gu, F.; Su, F. A thermodynamic analysis of methanation reactions of carbon oxides for the production of synthetic natural gas. *RSC Adv.* **2012**, *2*, 2358–2368. <https://doi.org/10.1039/c2ra00632d>.
7. Bailera, M.; Lisbona, P.; Romeo, L.M. Power to gas-oxyfuel boiler hybrid systems. *Int. J. Hydrog. Energy* **2015**, *40*, 10168–10175. <https://doi.org/10.1016/j.ijhydene.2015.06.074>.
8. Romeo, L.M.; Bailera, M. Design configurations to achieve an effective CO₂ use and mitigation through power to gas. *J. CO₂ Util.* **2020**, *39*, 1–10. <https://doi.org/10.1016/j.jcou.2020.101174>.
9. Bailera, M.; Hanak, D.P.; Lisbona, P.; Romeo, L.M. Techno-economic feasibility of power to gas-oxy-fuel boiler hybrid system under uncertainty. *Int. J. Hydrogen Energy* **2019**, *4*, 9505–9516. <https://doi.org/10.1016/j.ijhydene.2018.09.131>.
10. Eveloy, V. Hybridization of solid oxide electrolysis-based power-to-methane with oxyfuel combustion and carbon dioxide utilization for energy storage. *Renew. Sustain. Energy Rev.* **2019**, *108*, 550–571. <https://doi.org/10.1016/j.rser.2019.02.027>.
11. Bailera, M.; Lisbona, P.; Peña, B.; Romeo, L.M. A review on CO₂ mitigation in the Iron and Steel industry through Power to X processes. *J. CO₂ Util.* **2021**, *46*, 101456. <https://doi.org/10.1016/j.jcou.2021.101456>.
12. Kirschen, M.; Risonarta, V.; Pfeifer, H. Energy efficiency and the influence of gas burners to the energy related carbon dioxide emissions of electric arc furnaces in steel industry. *Energy* **2009**, *34*, 1065–1072. <https://doi.org/10.1016/j.energy.2009.04.015>.
13. Rosenfeld, D.C.; Böhm, H.; Lindorfer, J.; Lehner, M. Scenario analysis of implementing a power-to-gas and biomass gasification system in an integrated steel plant: A techno-economic and environmental study. *Renew. Energy* **2020**, *147*, 1511–1524. <https://doi.org/10.1016/j.renene.2019.09.053>.
14. Steelmaking technologies. CISDI ingeniering CO. LTD. Available online: <http://www.cisdigroup.com/4-steelmaking.html>. (accessed on 15 September 2021).
15. He, H.; Guan, H.; Zhu, X.; Lee, H. Assessment on the energy flow and carbon emissions of integrated steelmaking plants. *Energy Rep.* **2017**, *3*, 29–36. <https://doi.org/10.1016/j.egypr.2017.01.001>.
16. Wu, J.; Wang, R.; Pu, G.; Qi, H. Integrated assessment of exergy, energy and carbon dioxide emissions in an iron and steel industrial network. *Appl. Energy* **2016**, *183*, 430–444. <https://doi.org/10.1016/j.apenergy.2016.08.192>.
17. Geerdes, M.; Chaigneau, R.; Lingardi, O.; Molenaar, R. van O.; R., S.Y.; Warren, J. *Modern Blast Furnace Ironmaking an Introduction*; IOS Press, Amsterdam, Netherlands: 2020; ISBN 978-1-64368-123-8.
18. Ariyama, T.; Sato, M.; Nouchi, T.; Takahashi, K. Evolution of blast furnace process toward reductant flexibility and carbon dioxide mitigation in steel works. *ISIJ Int.* **2016**, *56*, 1681–1696. <https://doi.org/10.2355/isijinternational.ISIJINT-2016-210>.
19. Fisher, L.V.; Barron, A.R. The recycling and reuse of steelmaking slags—A review. *Resour. Conserv. Recycl.* **2019**, *146*, 244–255. <https://doi.org/10.1016/j.resconrec.2019.03.010>.
20. Darde, A.; Prabhakar, R.; Tranier, J.P.; Perrin, N. Air separation and flue gas compression and purification units for oxy-coal combustion systems. *Energy Procedia* **2009**, *1*, 527–534. <https://doi.org/10.1016/j.egypro.2009.01.070>.
21. Rönisch, S.; Schneider, J.; Matthischke, S.; Schlüter, M.; Götz, M.; Lefebvre, J.; Prabhakaran, P.; Bajohr, S. Review on methanation—From fundamentals to current projects. *Fuel* **2016**, *166*, 276–296. <https://doi.org/10.1016/j.fuel.2015.10.111>.
22. Biswas, A.K. *Principles of Blast Furnace Ironmaking. Theory and Practice*; Cootha Publishing House, Brisbane, Australia: 1981.
23. IAE—Iron & Steel Roadmap. 2020. Available online: <https://www.iea.org/reports/iron-and-steel-technology-roadmap> (accessed on 24 October 2021).
24. ITM Power to study feasibility of 100 MW P2G energy storage. *Fuel Cells Bull.* **2018**, *2018*, 11. [https://doi.org/10.1016/s1464-2859\(18\)30379-1](https://doi.org/10.1016/s1464-2859(18)30379-1).
25. Arasto, A.; Tsupari, E.; Kärki, J.; Pisilä, E.; Sorsamäki, L. Post-combustion capture of CO₂ at an integrated steel mill—Part I: Technical concept analysis. *Int. J. Greenh. Gas Control* **2013**, *16*, 271–277. <https://doi.org/10.1016/j.ijggc.2012.08.018>.
26. Tobiesen, F.A.; Svendsen, H.F.; Mejdell, T. Modeling of blast furnace CO₂ capture using amine absorbents. *Ind. Eng. Chem. Res.* **2007**, *46*, 7811–7819. <https://doi.org/10.1021/ie061556j>.
27. Keys, A.; van Hout, M.; Daniels, B. *Decarbonisation Options for the Dutch Steel Industry*; PBL Netherlands Environmental Assessment Agency, The Hague, Netherlands, 2019.
28. Zuo, G.; Hirsch, A. The trial of the Top Gas Recycling Blast Furnace at LKAB’s EBF and Scale-Up. *La Rev. Métallurgie* **2009**, *2*, 255.

29. Danloy, G.; Berthelemot, A.; Grant, M.; Borlée, J.; Sert, D.; van der Stel, J.; Jak, H.; Dimastromatteo, V.; Hallin, M.; Eklund, N.; et al. ULCOS—Pilot testing of the low-CO₂ Blast Furnace process at the experimental BF in Lulea. *Rev. Metall. Cah. D'Informations Tech.* **2009**, *106*, 1–8. <https://doi.org/10.1051/metal/2009008>.
30. Zhang, W.; Dai, J.; Li, C.; Yu, X.; Xue, Z.; Saxén, H. A Review on Explorations of the Oxygen Blast Furnace Process. *Steel Res. Int.* **2021**, *92*. <https://doi.org/10.1002/srin.202000326>.
31. Bailera, M.; Lisbona, P.; Peña, B.; Romeo, L.M. *Energy Storage*; Springer International Publishing: Cham, Switzerland, 2020; ISBN 978-3-030-46526-1.